Morphologic Choroidal and Scleral Changes at the Macula in Tilted Disc Syndrome with Staphyloma Using Optical Coherence Tomography

Ichiro Maruko, Tomohiro Iida, Yukinori Sugano, Hiroshi Oyamada, and Tetsuju Sekiryu

Purpose. To evaluate the macular choroidal and scleral changes in tilted disc syndrome (TDS) with staphyloma using optical coherence tomography (OCT) to determine the mechanism of serous retinal detachment (SRD) formation.

Methods. All eyes underwent fluorescein (FA) and indocyanine green angiography (ICGA) in this retrospective, observational study. Enhanced-depth imaging (EDI) OCT and prototype high-penetration (HP) OCT were used to examine the choroid and sclera, respectively, at the upper and lower optical areas and the subfovea on vertical OCT sections.

Results. Twenty-four eyes with TDS with inferior staphyloma were included. FA showed the macular area with the superior edge of staphyloma had a granular hyperfluorescent pattern and ICGA showed belt-like hypofluorescence. OCT showed SRDs in seven eyes. The mean EDI-OCT choroidal thicknesses in 19 eyes were: upper area, 211 ± 79 μm; subfovea, 153 ± 70 μm; and lower area, 158 ± 42 μm. The mean subfoveal and lower choroid were significantly ($P < 0.01$ for both) thinner than the upper area. The mean HP-OCT scleral thicknesses in 14 eyes were: upper area, 414 ± 36 μm; subfovea, 493 ± 40 μm; and lower area, 398 ± 83 μm. The subfoveal sclera was significantly ($P < 0.01$) thicker than the others.

Conclusions. The subfoveal choroid was relatively thin and the subfoveal sclera thickened in TDS with a staphyloma edge at the macula. The area with retinal pigment epithelial (RPE) atrophy was hyperfluorescent on FA; choriocapillaris occlusion was hypofluorescent on ICGA. Characteristic anatomic subfoveal scleral alterations might lead to a thinner choroid and inhibit chorioscleral outflow; a secondary RPE disorder subsequently could cause SRDs. (*Invest Ophthalmol Vis Sci.* 2011; 52:8763–8768) DOI:10.1167/iovs.11-8195

Although the tilted disc syndrome (TDS) usually is associated with good visual prognosis, foveal complications, such as serous retinal detachment (SRD), have been reported.[1–7] Staphyloma in TDS often is observed in the inferior ocular area, and the superior edge of the staphyloma sometimes involves the macula.[6,8–12] The superior edge of the inferior staphyloma at the fovea in TDS is characterized by a window defect on fluorescein angiography (FA) due to retinal pigment epithelial (RPE) atrophy and hypofluorescence due to choriocapillaris occlusion on indocyanine green angiography (ICGA).[6] These anatomic changes at the superior edge of the staphyloma might lead to foveal weakness and subsequent complications. Choroidal neovascularization (CNV) or polypoidal choroidal vasculopathy (PCV) in TDS was also reported as one of the complications due to anatomic changes at the macula area.[6,13]

Optical coherence tomography (OCT) is a noninvasive, advanced imaging technique for viewing the fovea that is critical for diagnosis and follow-up. In fact, SRDs at the fovea in TDS were clearly visualized by OCT for the first time.[3,4] Spectral-domain OCT (SD-OCT) is a high-speed, high-resolution technology that provides detailed images of the retinal structures in a short time. However, no study has investigated the choroidal and scleral changes in TDS using SD-OCT.

A new method for visualizing the choroid, enhanced-depth imaging OCT (EDI-OCT), was reported.[14] EDI-OCT can visualize the sclera in cases with a thinner retina and choroid, such as in pathologic myopia.[15] High-penetration OCT (HP-OCT) is another way to observe the choroid using a 1-μm wavelength.[16–20] Although the device is not commercially available, it is expected to visualize both the choroid and sclera.

The present study evaluated the choroidal and scleral changes using EDI-OCT or HP-OCT to elucidate the mechanism of SRD development in TDS with the superior edge of staphyloma at the fovea.

Methods

This retrospective study followed the tenets of the Declaration of Helsinki. The institutional review board at Fukushima Medical University School of Medicine approved this study that included OCT observation of eyes with macular and retinal disorders, observational study of age-related macular degeneration and similar disorders (including TDS), and use of the prototype HP-OCT not commercially available.

The present study involved the characteristic inferonasal tilting of the oval optic disc with a congenital inferonasal crescent with the superior edge of staphyloma at the fovea. The clinical examinations to diagnose TDS included measurement of the best-corrected visual acuity (BCVA), slit-lamp biomicroscopy with a contact or noncontact lens, indirect ophthalmoscopy, and digital FA and ICGA (TRC-50IX/IMAGEnet H1024 system, Topcon, Tokyo, Japan). The BCVA was measured with a Japanese standard decimal visual chart, and the logarithm of the minimum angle of resolution (logMAR) scale was used for statistical analysis. The spherical equivalent (SE) refractive error using an auto refractometer (Nidek, Gamagori, Japan) and the axial length using a biometer (IOL-Master; Carl Zeiss Meditec, Dublin, CA) were measured. Most eyes were examined with a commercially-available optical coherence tomograph (Heidelberg Spectralis; Heidelberg Engineering, Heidelberg, Germany) and the prototype HP-OCT with the 1060-nm wavelength (Topcon, Tokyo, Japan).

EDI-OCT

We observed the choroid, defined as the area between the outer RPE surface and the inner scleral surface, on vertical sections using EDI-

From the Department of Ophthalmology, Fukushima Medical University School of Medicine, Fukushima, Japan.

Submitted for publication July 10, 2011; revised September 19 and October 2, 2011; accepted October 2, 2011.

Disclosure: **I. Maruko**, None; **T. Iida**, None; **Y. Sugano**, None; **H. Oyamada**, None; **T. Sekiryu**, None

Corresponding author: Ichiro Maruko, Department of Ophthalmology, Fukushima Medical University School of Medicine, 1 Hikarigaoka, Fukushima, Japan; imaruko@fmu.ac.jp.

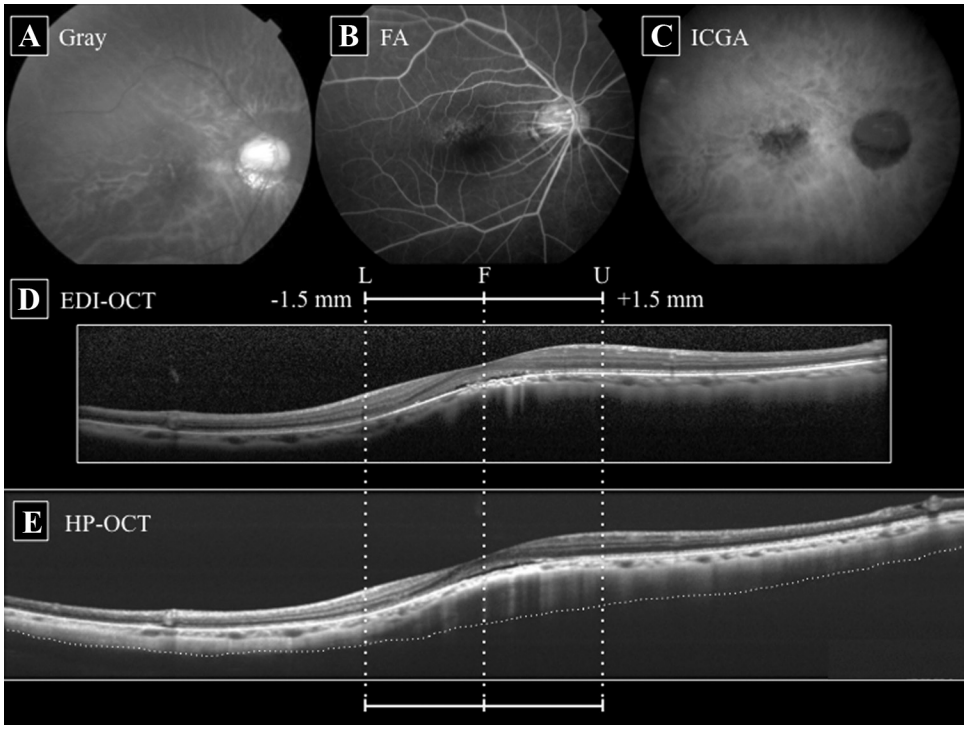

Figure 1. A 67-year-old woman (patient 3) has TDS in the right eye. The BCVA is 0.50 (20/40 Snellen; 0.30 logMAR), and the spherical equivalence is −15.25 diopters. The axial length is 27.33 mm. (**A**) A grayscale fundus photograph of the right eye shows the tilted optic disc with a crescent border and staphyloma from the inferior disc. (**B**) FA in the right eye shows the granular pattern of the hyperfluorescence at the macular area with a superior edge of staphyloma. (**C**) Late-phase ICGA shows belt-like hypofluorescence larger than the hyperfluorescence on FA. (**D**) EDI-OCT images show that the choroidal thickness on vertical section is 119 μm at the upper area (U), 93 μm at the subfovea (F), and 144 μm at the lower area (L). (**E**) The prototype HP-OCT shows that the choroidal thicknesses on vertical section are 116 μm at the upper area (U), 73 μm at the subfovea (F), and 139 μm at the lower area (L). The scleral thicknesses on a vertical section are 387 μm at the upper area (U), 480 μm at the subfovea (F), and 169 μm at the lower area (L). The *dotted line* indicates the posterior edge of the sclera defined as the hyperreflective area.

OCT,[14] in which the OCT device (Heidelberg Spectralis) is positioned close to the eye to obtain an inverted image. Each section was obtained using eye tracking, and 100 scans were averaged to improve the signal-to-noise ratio. The standard scanning length can be 9 mm. We measured the choroidal thicknesses at the subfovea and the upper and lower points 1.5 mm from the foveal depression on the vertical OCT lines passing through the fovea (EDI-OCT) (Figs. 1, 2).

Prototype HP-OCT

We observed the choroid on vertical sections and the sclera, defined as the hyperreflective area from the inner scleral surface, using HP-OCT. This instrument can average up to 50 images to improve the signal-to-noise ratio and enhance the choroid and sclera by movement of the reference mirror to change the focus similar to EDI-OCT when positioned close to the eye. When the full-thickness sclera could not be observed, the deepest hyperreflective point was used as the measurement value. No-reflection as the dark area behind the scleral hyperreflection was recognized as the existence of the different structures including the connecting tissues, vessels, muscles, or orbital fat. The standard scanning length can be 12 mm, which is longer than the scanning length with EDI-OCT. We measured the choroidal and scleral thicknesses at the subfovea and the upper and lower points 1.5 mm

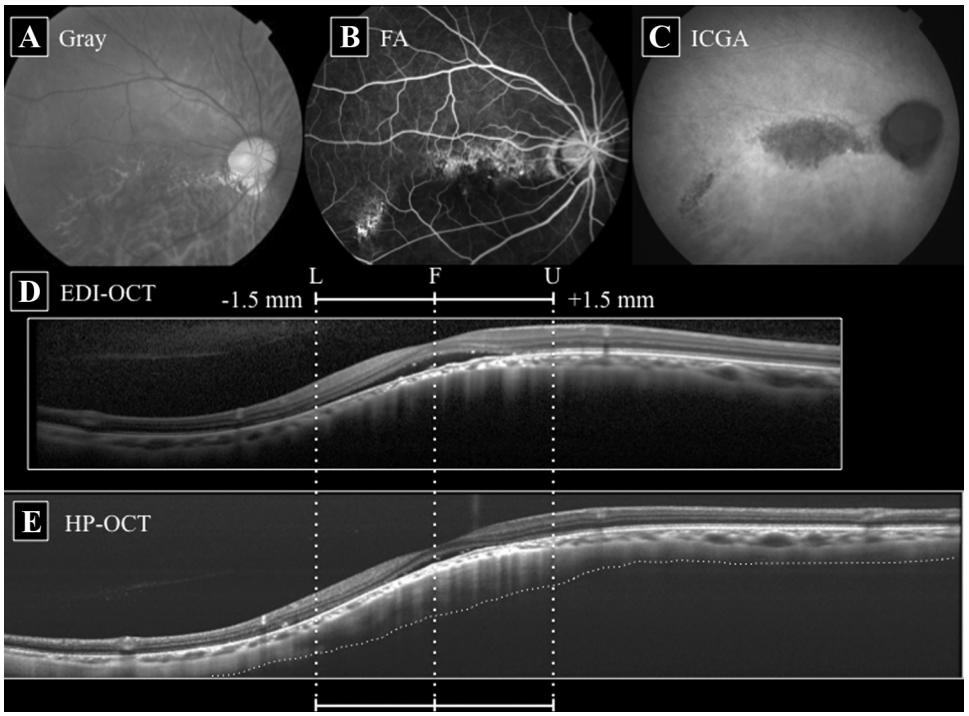

Figure 2. A 45-year-old man (patient 7) with TDS in the right eye. The BCVA is 0.30 (20/67 Snellen; 0.52 logMAR), and the spherical equivalence is −3.875 diopters. The axial length is 24.56 mm. (**A**) A grayscale fundus photograph of the right eye shows the tilted optic disc with a crescent border and staphyloma from the inferior disc. (**B**) FA in the right eye shows slight hyperfluorescence at the macular area with the superior edge of staphyloma. (**C**) Late-phase ICGA shows belt-like hypofluorescence larger than the hyperfluorescence on FA. (**D**) An EDI-OCT image shows that the choroidal thicknesses on vertical section are 151 μm at the upper area (U), 98 μm at the subfovea (F), and 124 μm at the lower area (L). (**E**) A prototype HP-OCT image shows that the choroidal thicknesses on vertical section are 146 μm at the upper area (U), 89 μm at the subfovea (F), and 122 μm at the lower area (L). The scleral thicknesses on vertical section are 449 μm at the upper area (U), 526 μm at the subfovea (F), and 468 μm at the lower area (L). The *dotted line* indicates the posterior edge of the sclera defined as the hyperreflective area.

from the foveal depression on the vertical OCT lines passing through the fovea (HP-OCT) (Figs. 1, 2).

The reported measurements obtained from the OCT images represented the average measurements obtained by three coauthors (IM, YS, HO). The visual acuities (VAs) are expressed as the decimal and logMAR equivalents, the standard Snellen VA values also were recorded. The results of the measurement of the choroidal and scleral thicknesses were analyzed using the Wilcoxon signed rank test. $P < 0.05$ was considered statistically significant.

Results

Twenty-four eyes of 13 patients (2 men, 11 women; mean age, 56.2 years) were diagnosed with TDS with the superior edge of staphyloma at the fovea. The optic disc in all cases was elevated to the upper (superotemporal) area, with a crescent at the inferior or inferonasal margin. The mean BCVA was 0.54 (20/37 Snellen; 0.27 logMAR), and the mean spherical equivalence (SE) was −4.47 diopters (D). All eyes underwent FA and ICGA. FA showed band-shaped granular hyperfluorescence corresponding to the atrophic band with the superior edge of staphyloma in all eyes. Early phase of ICGA showed an asymmetric choroidal vascular pattern between the upper and the lower fundus across the superior edge of staphyloma. In the inferior staphyloma, less number and smaller caliber of the choroidal vessels were delineated in ICGA. The superior border of the inferior staphyloma showed band-shaped hypofluorescence during ICGA throughout the angiographic phase. The band-shaped hypofluorescent area on late-phase of ICGA was larger than that of the hyperfluorescence seen on FA. There was no lesion suggestive of CNV or PCV in the present study. Figures 1 and 2 show representative cases of TDS with the superior edge of staphyloma at the fovea. Table 1 shows the patient data including the choroidal and scleral thicknesses.

Among all cases, 19 eyes of 10 patients were examined using EDI-OCT. Seven eyes had an SRD. The mean axial length was 25.05 ± 1.26 mm. The mean choroidal thickness on the vertical EDI-OCT images was 211 ± 79 μm at the upper area, 153 ± 70 μm at the subfovea, and 158 ± 42 μm at the lower area. The mean choroidal thicknesses at the subfovea and the lower area were significantly ($P < 0.01$, for both comparisons) thinner than the upper area. The mean subfoveal choroidal thickness in eyes with an SRD was slightly thicker than in eyes without an SRD; however, the difference was not significant (176 ± 80 μm; 140 ± 63 μm; $P = 0.27$).

Fourteen eyes of nine patients were observed with EDI-OCT and HP-OCT. Seven eyes had an SRD. The mean axial length was 24.89 ± 1.05 mm. The mean choroidal thicknesses on EDI-OCT vertical sections were 212 ± 87 μm at the upper area, 148 ± 76 μm at the subfovea, and 154 ± 43 μm at the lower area. The mean choroidal thicknesses on the vertical HP-OCT images were 211 ± 91 μm at the upper area, 144 ± 81 μm at the subfovea, and 156 ± 49 μm at the lower area. The data at the three points from EDI- or HP-OCT were almost the same, and there was no significant difference ($P = 0.61$ at the upper area; $P = 0.49$ at the subfovea; $P = 0.88$ at the lower area). The mean subfoveal choroidal thicknesses in eyes with an SRD were slightly thicker than in eyes without an SRD on EDI-OCT (176 ± 80 μm and 119 ± 65 μm, respectively; $P = 0.08$). The mean subfoveal choroidal thicknesses in eyes with an SRD were slightly thicker than in eyes without an SRD on HP-OCT (174 ± 92 μm and 115 ± 62 μm, respectively; $P = 0.27$). The mean scleral thicknesses on vertical HP-OCT images were 414 ± 36 μm at the upper area, 493 ± 40 μm at the subfovea, and 398 ± 83 μm at the lower area. The subfoveal sclera was significantly thicker than the other structures ($P < 0.01$, for both comparisons). Full thickness sclera was observed at the outside of the foveal area in all 14 eyes, and measurement values defined as the deepest hyperreflective point at the subfovea were thicker than at the outside of the foveal area even in eyes with invisible full thickness sclera at the foveal area. There was no significant difference between the mean subfoveal scleral thickness on HP-OCT in eyes with and without an SRD (481 ± 45 μm and 505 ± 33 μm, respectively; $P = 0.34$).

Discussion

In the present study, the subfoveal choroid was thinner than that in the outside area of staphyloma, and the subfoveal sclera was thicker than that in the other areas. The characteristic anatomic changes including the subfoveal scleral thickening in TDS might induce choroidal thinning and abnormal choroidal circulation at the fovea; secondary RPE atrophy could cause breakdown of the blood-retinal barrier and a subsequent SRD.

In the present study for TDS, HP-OCT showed almost the same choroidal measurements as EDI-OCT. Ikuno et al.[21] reported the reproducibility of choroidal thickness using both EDI-OCT and HP-OCT devices. Intersystem intraclass correlation coefficient showed the high correlation values of 0.921. Thus, both OCT systems can evaluate the choroidal thickness measurements as the same values, and these are also proved in eyes with TDS.

In patients with TDS, moderate myopia is common.[22] The present study supported this (e.g., the mean spherical equivalence was −4.5 diopters and the mean axial length was 25 mm). Lacquer cracks, representing breaks in Bruch's membrane, are sometimes seen in the posterior pole in eyes with pathologic myopia.[23,24] FA showed hyperfluorescence and ICGA showed well-delineated hypofluorescence corresponding to the lacquer cracks.[23] These angiographic features of the lacquer cracks in eyes with pathologic myopia are similar to those of the superior edge of staphyloma in TDS. In the present study, FA showed the hyperfluorescence and ICGA showed the hypofluorescence at the superior border of the inferior staphyloma in all cases. These may indicate less number and smaller caliber of choroidal vessels and subsequent ischemic changes at the staphyloma edge provide RPE atrophy. Thus, the chorioretinal expansion of the staphyloma may lead to RPE atrophy in TDS. However, a macular hole retinal detachment, retinal schisis, simple subretinal hemorrhage, and even lacquer cracks were not commonly observed in TDS. This may indicate that another mechanism of myopia is associated with the pathophysiology of TDS.

Recently, a new method to visualize the choroid, EDI-OCT, was described.[14] Margolis and Spaide[25] reported that the subfoveal choroidal thickness in normal subjects was 287 μm. We reported a subfoveal choroidal thickness of 250 μm.[26] Fujiwara et al.[27] reported that the subfoveal choroidal thickness in highly myopic eyes was 93.2 μm. In the present study, the subfoveal choroidal thickness in TDS was 153 μm on EDI-OCT, which might indicate that the subfoveal choroidal thickness in TDS is thinner than in normal eyes and thicker than in highly myopic eyes. Subfoveal choroidal thickness in typical central serous chorioretinopathy (CSC) has been reported to be thicker than normal in recent EDI-OCT studies.[26,28] In the present study, the subfoveal choroid was not thick in eyes with TDS, however subfoveal choroid in seven eyes with an SRD was slightly, but not significantly, thicker than in eyes without a detachment in TDS. Although FA did not show focal leakage in TDS, the choroidal fluid may flow from the choroid to the subretina through the damaged RPE. Thus, the pathophysiology of SRDs in TDS may not be identical with that in CSC, but there can be some similarities.

Table 1. Clinical Characteristics of Patients with Tilted Disc Syndrome in the Current Study

Patient Number	Eye Number	OD/OS	Sex	Age (y)	BCVA (logMAR)	SE, D	Axial Length (mm)	SRD	Choroidal Thickness on EDI-OCT (μm)			Choroidal Thickness on HP-OCT (μm)			Scleral Thickness on HP-OCT (μm)		
									Upper	Subfovea	Lower	Upper	Subfovea	Lower	Upper	Subfovea	Lower
1	1	OD	F	44.4	1.00 (0.00)	−1.875	23.50	−	207	90	124	203	84	105	443	516	431
	2	OS			0.60 (0.22)	−2.375	23.60	+	170	112	122	175	103	127	354	483	386
2	3	OD	F	39.5	0.20 (0.70)	−2.125	24.33	+	310	240	114	298	223	124	430	462	495
	4	OS			1.50 (−0.18)	−0.875	24.21	+	375	279	191	396	283	217	392	396	373
3	5	OD	F	67.2	0.50 (0.30)	−15.250	27.33	+	119	93	144	116	73	139	387	480	169
4	6	OD			0.80 (0.10)	−5.625	26.23	−	139	89	123	139	83	122	354	445	310
	7	OS	F	65.5	1.00 (0.00)	−5.250	25.78	−	149	91	136	149	89	138	424	474	354
5	8	OD			0.60 (0.22)	−3.375	24.79	−	207	84	148	197	97	125	386	531	392
	9	OS	F	59.7	0.60 (0.22)	−3.500	24.10	−	178	103	171	162	100	164	455	526	436
6	10	OD			0.50 (0.30)	−5.750	25.60	−	335	265	226	308	254	222	474	506	398
	11	OS	M	44.0	0.20 (0.70)	−4.500	24.77	+	329	257	247	357	292	275	424	492	468
7	12	OD			0.30 (0.52)	−3.875	24.56	+	151	98	124	146	89	122	449	526	468
	13	OS	M	45.1	1.50 (−0.18)	−1.125	23.86	−	210	189	168	NA	NA	NA	NA	NA	NA
8	14	OD			0.90 (0.05)	−2.750	25.03	−	130	112	112	121	98	127	417	535	430
	15	OS	F	67.9	0.50 (0.30)	−11.500	28.06	−	221	178	147	NA	NA	NA	NA	NA	NA
9	16	OD			0.60 (0.22)	−4.500	24.69	+	165	154	174	184	154	172	411	529	462
	17	OS	F	39.6	1.50 (−0.18)	−2.375	23.94	−	297	241	218	NA	NA	NA	NA	NA	NA
10	18	OD			1.00 (0.00)	−9.375	26.57	−	153	127	114	NA	NA	NA	NA	NA	NA
	19	OS	F	59.0	0.70 (0.15)	−5.000	24.93	−	166	106	199	NA	NA	NA	NA	NA	NA
11	20	OD			0.50 (0.30)	−5.250	NA	NA	NA	NA	NA	NA	NA	NA	NA	NA	NA
	21	OS	F	69.5	0.50 (0.30)	−1.125	NA	NA	NA	NA	NA	NA	NA	NA	NA	NA	NA
12	22	OD			0.10 (1.00)	1.875	NA	NA	NA	NA	NA	NA	NA	NA	NA	NA	NA
	23	OS	F	69.0	0.10 (1.00)	−5.500	NA	NA	NA	NA	NA	NA	NA	NA	NA	NA	NA
13	24	OD	F	60.0	0.50 (0.30)	−6.375	NA	NA	NA	NA	NA	NA	NA	NA	NA	NA	NA
Mean*			M 2:F 11	56.2	0.69 (0.16)	−4.47	25.05 (1.26)	7	211 (79)	153 (70)	158 (42)	211 (87)	144 (81)	156 (49)	414 (36)	493 (40)	398 (83)

Choroidal and scleral thicknesses are measured at the subfovea, upper, and lower points of 1.5 mm from the foveal depression. F, female; M, male; NA, not available.
*Values are mean (SD) except for BCVA (logMAR), and Sex, and SRD, which are totals.

A dome-shaped macula is characterized by a convex protrusion of the macula within the staphyloma in highly myopic eyes seen on OCT. Gaucher et al.[29] reported that an SRD was present in 67% (10/15 eyes) of eyes with a dome-shaped macula using conventional (Stratus) OCT (Carl Zeiss Meditec, Inc, Dublin, CA). Imamura et al.[15] evaluated the posterior anatomic structure of dome-shaped maculas using EDI-OCT and reported subfoveal choroidal thinning and subfoveal scleral thickening. Although the sclera can be observed by EDI-OCT in eyes with a thinner retina and choroid in patients with a dome-shaped macula associated with pathologic myopia, it is difficult to evaluate the sclera in cases with TDS with relative myopia on EDI-OCT.

Because HP-OCT has a wavelength that is 1 μm longer than the commercially-available device, HP-OCT is expected to visualize not only the choroid but also the sclera in non-myopic eyes. Using the prototype HP-OCT, the subfoveal sclera in cases of TDS was significantly thicker than the other areas. These results may be similar to scleral thickening in patients with a dome-shaped macula even though the pathogenic mechanisms and clinical conditions differ.

We recognize there are two types of diseases with SRD at the fovea; one is the disease with choroidal thickening such as CSC[26,28] and Vogt-Koyanagi-Harada disease,[30] and the other is the disease with choroidal thinning such as a dome-shaped macula[15] associated with highly myopic eyes. The former is definitely associated with choroidal abnormalities of choroidal vascular hyperpermeability or inflammatory infiltration. Because the choroid in TDS was thin and choroidal vascular hyperpermeability was not observed on ICGA, the choroid might not be contributed to SRD in TDS. The latter is not fully understood. Imamura et al.[15] reported that subretinal fluid in patients with a dome-shaped macula might accumulate because of impaired choroidal outflow resulting from scleral thickening. We think the similar mechanism to the dome-shaped macula occurs around the foveal area in TDS, thus the choroidal fluid in TDS might not pass through a thickened sclera and could leak into the subretina through the degenerated RPE seen on angiography. Although the subfoveal choroid in eyes with SRD was relatively thicker than in eyes without SRD, the choroidal fluid in TDS with SRD might be partially stored in the choroid because of the obstruction of choroidal outflow. The mechanism of SRD development in TDS might be completely different from CSC.

In the present study, EDI-OCT and HP-OCT showed that the subfoveal choroid was thinner than in the outside area of staphyloma and the subfoveal sclera was thicker than in other areas. Choroidal outflow obstruction and RPE damage seen on OCT and angiography might induce subsequent SRDs. Several limitations of the present study included its retrospective design and the small number of patients. CNV or PCV in TDS is sometimes observed as a complication.[6,13] Although we do not have such a case with CNV or PCV in the present study, it is important enough to cause the visual loss in TDS. Further study will need to elucidate the pathogenesis of CNV or PCV in TDS. Nevertheless, no previous study has visualized the choroid and sclera in TDS using EDI-OCT and HP-OCT.

Acknowledgments

The authors thank Masahiro Akiba from Topcon Corp. (Tokyo, Japan) for providing a prototype high penetration optical coherence tomography instrument.

References

1. Cohen SY, Quentel G, Guiberteau B, Delahaye-Mazza C, Gaudric A. Macular serous retinal detachment caused by subretinal leakage in tilted disc syndrome. *Ophthalmology.* 1998;105:1831–1834.
2. Tosti G. Serous macular detachment and tilted disc syndrome. *Ophthalmology.* 1999;106:1453–1455.
3. Leys AM, Cohen SY. Subretinal leakage in myopic eyes with a posterior staphyloma or tilted disk syndrome. *Retina.* 2002;22:659–665.
4. Theodossiadis PG, Grigoropoulos V, Emfietzoglou J, Theodossiadis GP. Optical coherence tomography study of tilted optic disk associated with macular detachment. *Graefes Arch Clin Exp Ophthalmol.* 2006;244:122–124.
5. Miura G, Yamamoto S, Tojo N, Mizunoya S. Foveal retinal detachment and retinoschisis without macular hole associated with tilted disc syndrome. *Jpn J Ophthalmol.* 2006;50:566–567.
6. Nakanishi H, Tsujikawa A, Gotoh N, et al. Macular complications on the border of an inferior staphyloma associated with tilted disc syndrome. *Retina.* 2008;28:1493–1501.
7. Milani P, Pece A, Pierro L, Seidenari P, Radice P, Scialdone A. Bevacizumab for macular serous neuroretinal detachment in tilted disk syndrome. *J Ophthalmol.* 2010;2010:970580.
8. Alexander LJ. The tilted disc syndrome. *J Am Optom Assoc.* 1978;49:1060–1062.
9. Sowka J, Aoun P. Tilted disc syndrome. *Optom Vis Sci.* 1999;76:618–623.
10. Quaranta M, Brindeau C, Coscas G, Soubrane G. Multiple choroidal neovascularizations at the border of a myopic posterior macular staphyloma. *Graefes Arch Clin Exp Ophthalmol.* 2000;238:101–103.
11. Cohen SY, Quentel G. Chorioretinal folds as a consequence of inferior staphyloma associated with tilted disc syndrome. *Graefes Arch Clin Exp Ophthalmol.* 2006;244:1536–1538.
12. Ohno-Matsui K, Shimada N, Nagaoka N, Tokoro T, Mochizuki M. Choroidal folds radiating from the edge of an inferior staphyloma in an eye with tilted disc syndrome. *Jpn J Ophthalmol.* 2011;55:171–173.
13. Mauget-Faÿsse M, Cornut PL, Quaranta El-Maftouhi M, Leys A. Polypoidal choroidal vasculopathy in tilted disk syndrome and high myopia with staphyloma. *Am J Ophthalmol.* 2006;142:970–975.
14. Spaide RF, Koizumi H, Pozzoni MC. Enhanced depth imaging spectral-domain optical coherence tomography. *Am J Ophthalmol.* 2008;146:496–500.
15. Imamura Y, Iida T, Maruko I, Zweifel SA, Spaide RF. Enhanced depth imaging optical coherence tomography of the sclera in dome-shaped macula. *Am J Ophthalmol.* 2011;151:297–302.
16. de Bruin DM, Burnes DL, Loewenstein J, et al. In-vivo three-dimensional imaging of neovascular age-related macular degeneration using optical frequency domain imaging at 1050 nm. *Invest Ophthalmol Vis Sci.* 2008;49:4545–4552.
17. Srinivasan VJ, Adler DC, Chen Y, et al. Ultrahigh-speed optical coherence tomography for three-dimensional and en face imaging of the retina and optic nerve head. *Invest Ophthalmol Vis Sci.* 2008;49:5103–5110.
18. Yasuno Y, Miura M, Kawana K, et al. Visualization of sub-retinal pigment epithelium morphologies of exudative macular diseases by high-penetration optical coherence tomography. *Invest Ophthalmol Vis Sci.* 2009;50:405–413.
19. Povazay B, Hermann B, Hofer B, et al. Wide-field optical coherence tomography of the choroid in vivo. *Invest Ophthalmol Vis Sci.* 2009;50:1856–1863.
20. Ikuno Y, Kawaguchi K, Nouchi T, Yasuno Y. Choroidal thickness in healthy Japanese subjects. *Invest Ophthalmol Vis Sci.* 2010;51:2173–2176.
21. Ikuno Y, Maruko I, Yasuno Y, et al. Reproducibility of retinal and choroidal thickness measurements in enhanced depth imaging and high-penetration optical coherence tomography. *Invest Ophthalmol Vis Sci.* 2011;52:5536–5540.
22. Young SE, Walsh FB, Knox DL. The tilted disk syndrome. *Am J Ophthalmol.* 1976;82:16–23.
23. Klein RM, Curtin BJ. Lacquer crack lesions in pathologic myopia. *Am J Ophthalmol.* 1975;79:386–392.
24. Klein RM, Green S. The development of lacquer cracks in pathologic myopia. *Am J Ophthalmol.* 1988;106:282–285.

25. Margolis R, Spaide RF. A pilot study of enhanced depth imaging optical coherence tomography of the choroid in normal eyes. *Am J Ophthalmol.* 2009;147:811–815.
26. Maruko I, Iida T, Sugano Y, Ojima A, Sekiryu T. Subfoveal choroidal thickness in fellow eyes of patients with central serous chorioretinopathy. *Retina.* 2011;31:1603–1608.
27. Fujiwara T, Imamura Y, Margolis R, Slakter JS, Spaide RF. Enhanced depth imaging optical coherence tomography of the choroid in highly myopic eyes. *Am J Ophthalmol.* 2009;148: 445–450.
28. Imamura Y, Fujiwara T, Margolis R, Spaide RF. Enhanced depth imaging optical coherence tomography of the choroid in central serous chorioretinopathy. *Retina.* 2009;29:1469-1473.
29. Gaucher D, Erginay A, Lecleire-Collet A, et al. Dome-shaped macula in eyes with myopic posterior staphyloma. *Am J Ophthalmol.* 2008;145:909–914.
30. Maruko I, Iida T, Sugano Y, et al. Subfoveal choroidal thickness after treatment of Vogt-Koyanagi-Harada disease. *Retina.* 2011;31: 510–517.